# Exact Diagonalization of the Hamiltonian for Trapped Interacting Bosons

Tor Haugset and Hårek Haugerud

Department of Physics

University of Oslo

N-0316 Oslo, Norway

**Abstract:** We consider systems of a small number of interacting bosons confined to harmonic potentials in one and two dimensions. By exact numerical diagonalization of the many-body Hamiltonian we determine the low lying excitation energies and the ground state energy and density profile. We discuss the dependence of these quantities on both interaction strength g and particle number N. The ground state properties are compared to the predictions of the Gross-Pitaevskii equation, which depends on these parameters only through the combination Ng. We also calculate the specific heat based on the obtained energy spectra.

PACS numbers: 05.30.Jp, 03.75.Fi, 67.40.Db, 32.80.Pj

### 1 Introduction

Recent observations of Bose-Einstein condensation in alkali gases confined to harmonic potentials [1, 2] has led to an extensive study of the ground state and low energy properties of trapped interacting Bose gases. A major part of this work, see e.g. [3, 4, 5, 6, 7, 8, 9], presents calculations based on the Bogoliubov approximation or Hartree-Fock theory. Predicted excitation frequencies agree well with experiments [10, 11]. The energy spectrum has also been described in terms of a hydrodynamic formalism [12], which agrees with Bogoliubov theory at low energy [8, 13]. In the Bogoliubov approximation the system is described in terms of a dominating condensate. Fluctuations induced by finite temperature and interactions are assumed small. At zero temperature, when the effects of excited particles are neglected, the condensate satisfies the Gross-Pitaevskii equation [14, 15, 16].

The Bogoliubov approximation is applicable for systems with a large number of particles. In this paper we will, on the contrary, consider systems with relatively few particles, i.e.  $N \sim 10-40$ . Finite N effects are then important, and one should in principle use the complete machinery of many-body theory when describing these systems. We here present the results of such calculations, limiting ourselves to one and two dimensions for the sake of simplicity. The higher

degree of degeneracy introduced by including yet another dimension will set an even lower limit on the number of particles for which one may in practice do calculations. The use of such time- and computer power consuming methods puts severe limitations on the size of the system one may describe. On the other hand, it is for such systems the corrections to mean-field calculations are important.

The results presented here are therefore not immediately relevant for the experiments performed with trapped Bose gases this far. Our aim is rather to gain some insight into the effects of the approximations which form the basis of the mean-field theories mentioned above, at least in the limit of small particle numbers. We will also discuss how one might include the effect of finite N in the mean field description. In addition, future experiments in lower dimensions may explore the range of parameters used here.

The plan of the article is as follows. In the next Section we recall the many-body formalism and describe the steps leading to the diagonalization of the many-body Hamiltonian. The Gross-Pitaevskii approximation, to which we compare our results for the ground state, is discussed in Section 3. Numerical results are presented and discussed in Section 4. Finally we draw some conclusions in the last section. The Appendix discusses effective couplings in highly anisotropic systems.

## 2 Many-body description

As a model for a trapped interacting Bose gas we study the Hamiltonian density

$$\mathcal{H} = \hat{\Psi}^{\dagger}(\mathbf{r}) \left[ -\frac{\nabla^2}{2m} + V_{ex}(\mathbf{r}) \right] \hat{\Psi}(\mathbf{r}) + \mathcal{H}_I(\hat{\Psi}^{\dagger}, \hat{\Psi}), \tag{1}$$

where  $\hat{\Psi}$  is a bosonic field operator and  $V_{ex}$  is the external trapping potential. Units where  $\hbar = 1$  are used. We will only consider isotropic harmonic potentials of the form  $V_{ex}(\mathbf{r}) = \frac{1}{2}m\omega^2 r^2$ .  $\mathcal{H}_I$  describes the interaction. Assuming short-range two-body interaction, this may be written

$$\mathcal{H}_{I} = q\hat{\Psi}^{\dagger}(\mathbf{r})\hat{\Psi}^{\dagger}(\mathbf{r})\hat{\Psi}(\mathbf{r})\hat{\Psi}(\mathbf{r}). \tag{2}$$

In the s-wave approximation the coupling constant, or interaction strength g is related to the scattering length a by the equation  $g = 2\pi a/m$  in three dimensions. In Appendix A we discuss modifications of this relation in highly anisotropic harmonic traps.

Harmonic modes. As a step towards finding the energy eigenvalues, we expand the field operator in a complete set of modes

$$\hat{\Psi}(\mathbf{r}) = \sum_{k} \phi_k(\mathbf{r}) a_k,\tag{3}$$

where  $a_k/a_k^{\dagger}$  annihilates/creates a particle in state k. The operators satisfy the commutation relation  $[a_k, a_l^{\dagger}] = \delta_{k,l}$ , with other commutators vanishing. In translation invariant systems it is convenient to choose a set of plane waves. Here it proves more efficient to use the Harmonic oscillator eigenfunctions. The Hamiltonian then takes the form

$$H \equiv \int d\mathbf{r} \mathcal{H} = \sum_{k} \omega_k a_k^{\dagger} a_k + g \sum_{k,l,m,n} f_{klmn} a_k^{\dagger} a_l^{\dagger} a_m a_n. \tag{4}$$

 $\omega_k$  is the single particle energy of level k, and  $f_{klmn}$  is an overlap integral over four oscillator eigenfunctions

$$f_{klmn} = \int d\mathbf{r} \phi_k^* \phi_l^* \phi_m \phi_n(\mathbf{r}). \tag{5}$$

For the complete set of eigenfunctions  $\{\phi_k\}$  we will choose Hermite or Laguerre polynomials for one and two dimensions respectively. The corresponding overlap integrals can be calculated numerically, though some of them are tabulated [17]. The interaction conserves parity. In one dimension this leads to the constraint k+l+m+n= even integer for non-zero f. In two dimensions the rotation symmetry of the external potential suggests the use of radial and angular quantum numbers. The interaction conserves angular momentum, and this again puts a constraint on the possible combinations of creation and annihilation operators.

Many particle basis and diagonalization. The Hamiltonian is diagonalized in a many particle basis, which in the occupation-number representation may be written in the form

$$|\psi_{\alpha}\rangle = |n_0 n_1 n_2 \cdots n_K\rangle_{\alpha},\tag{6}$$

with  $\alpha$  labeling the different distributions of particles. Normalization to unity is assumed. Here  $n_k$  is the particle number in the single particle state k. The particle number is conserved:  $\sum_k n_k = N$ . In a concrete calculation we must truncate the basis set at some upper state, here denoted by K. This sets an upper limit for the single particle energy of the states considered. Such a truncation is however somewhat unnatural as far as the many particle energy is concerned, since it will include the many particle state  $|N_K\rangle$  with energy  $N\omega_K$ , but not the state  $|(N-1)_01_{K+1}\rangle$  which only has energy  $\omega_{K+1} + (N-1)\omega_0$ . A more consistent way of truncating the basis set is therefore to include only those states which have a total energy up to some maximal value  $E_{max}$ . In the actual calculation,  $E_{max}$  will be raised in steps until convergence is reached. The creation and annihilation operators have the usual effect on these states:

$$a_k | n_0 \cdots n_K \rangle = \sqrt{n_k} | n_0 \cdots n_k - 1 \cdots n_K \rangle$$

$$a_k^{\dagger} | n_0 \cdots n_K \rangle = \sqrt{n_k + 1} | n_0 \cdots n_k + 1 \cdots n_K \rangle. \tag{7}$$

The number operator is thus  $a_k^{\dagger} a_k$  with eigenvalue  $n_k$ .

With a basis set at hand, we may calculate the Hamiltonian matrix elements

$$H_{\alpha',\alpha} = \langle \psi_{\alpha'} | H | \psi_{\alpha} \rangle = H_{0\alpha} \delta_{\alpha',\alpha} + H_{I\alpha',\alpha}. \tag{8}$$

The free part of the Hamiltonian contributes to the diagonal terms with an amount  $\sum_k \omega_k n_k$ , while the interaction part yields the contribution

$$g \sum_{k,l,m,n} f_{klmn} \langle \psi_{\alpha'} | a_k^{\dagger} a_l^{\dagger} a_m a_n | \psi_{\alpha} \rangle. \tag{9}$$

The symmetries of the interaction can be used to reduce the Hamiltonian matrix to a block diagonal form. Splitting the complete Fock space into several symmetry invariant subspaces reduces the dimensions of the Hamiltonian matrix considerably and enables numerical diagonalization of much larger systems. In one dimension there is an even and an odd parity subspace and the ground state is a superposition of even parity states. In two dimensions the subspaces are labeled by the total angular momentum of the many particle state and the ground state has zero angular momentum.

The Hamiltonian matrix is relatively sparse and the iterative Lanczos method [18] is thus well suited for finding the groundstate and the lowest excited states. This method enables us to diagonalize much larger matrices than would be possible with standard library routines. However, we use the latter when finding the complete set of energy levels needed for calculating thermodynamic quantities.

Density profile. Once the Hamiltonian is diagonalized, we have the coefficients for the low lying states, and especially for the ground state. This enables us to find the ground state density distribution  $\rho(\mathbf{r})$ . The density operator may be written

$$\hat{n}_{\psi} = \sum_{k,l} |k\rangle n_{kl} \langle l|, \tag{10}$$

where  $|k\rangle$  is a single particle state, and  $n_{kl} = \langle \psi | a_l^{\dagger} a_k | \psi \rangle$ . The density is then  $\rho(\mathbf{r}) = \langle \mathbf{r} | \hat{n}_{\psi} | \mathbf{r} \rangle$ . For a state  $|\psi\rangle = \sum_{\alpha} C_{\alpha} |\psi_{\alpha}\rangle$  this reads

$$\rho(\mathbf{r}) = \sum_{k,l} \phi_l^* \phi_k(\mathbf{r}) \sum_{\alpha,\alpha'} C_{\alpha'}^* C_{\alpha} \langle \psi_{\alpha'} | a_l^{\dagger} a_k | \psi_{\alpha} \rangle.$$
 (11)

Dipole mode. The excitations in this system will in general have interaction dependent energies. However, as discussed by Fetter and Rokhsar [13], there exists a dipole mode for each spatial dimension of the trap, which corresponds to a harmonic oscillation of the center of mass of the condensate. In [13] the corresponding raising operator was constructed in the first quantized formalism:

$$A_{\beta}^{\dagger} = \sum_{i}^{N} b_{\beta i}^{\dagger},\tag{12}$$

where  $b_{\beta i}^{\dagger}$  is the raising operator for particle number i in dimension  $\beta$ . (We use a different notation than in [13], in order to avoid confusion with quantities defined in the present paper.) With a two-body potential of the form  $V(\mathbf{r}_i - \mathbf{r}_j)$  it is easily shown that the excitation energy is  $\omega$ , i.e. independent of the interaction. Thus, for each energy level there must be a ladder of levels with energy spacing  $\omega$  above. These dipole modes have been found in calculations based on the Bogoliubov approximation [4, 7] and in the hydrodynamic description [12]. The occurrence of these states will serve as a check of convergence of the calculated energy levels. For completeness we note that the raising operator in terms of creation and annihilation operators in one dimension takes the form

$$A^{\dagger} = \sum_{k} \sqrt{k+1} a_{k+1}^{\dagger} a_k. \tag{13}$$

Here k labels the Hermite polynomials. Commuting the raising operator with the free particle Hamiltonian we find

$$[H_0, A^{\dagger}] = \omega A^{\dagger}, \tag{14}$$

and the excitation energy is thus  $\omega$ . The vanishing of the commutator of  $A^{\dagger}$  with the interaction term is less obvious in this formalism. The commutator becomes

$$[H_I, A^{\dagger}] = 2g \sum_{k,l,m,n} a_k^{\dagger} \sqrt{l+1} (f_{kmnl+1} a_n^{\dagger} a_l - f_{kmnl} a_{l+1}^{\dagger} a_n) a_m, \tag{15}$$

and for each combination  $a_k^{\dagger} a_l^{\dagger} a_m a_n$  the prefactor vanishes. This is due to the following relation between the overlap integrals:

$$\sqrt{d+1}f_{abcd+1} + \sqrt{c+1}f_{abc+1d} = \sqrt{a}f_{a-1bcd} + \sqrt{b}f_{ab-1cd}.$$
 (16)

Exact Solution. It should be mentioned that the one-dimensional, homogeneous Bose gas with  $\delta$ -function interaction is one of a few systems which may be solved exactly applying the Bethe ansatz [19, 20, 21]. However, to our knowledge the exists no exact solution in the presence of an external trapping potential.

## 3 Mean field Approximation

One of the purposes of this paper is to compare the predictions of the many-body calculation with those of mean field theory for quantities such as the ground state energy and density distribution. The condensate is in the Gross-Pitaevskii (GP) approximation [14, 15] described by a classical, macroscopic Bose field governed by the Hamiltonian density per particle

$$\mathcal{H}_{cl}/N = \Phi^*(\mathbf{r}) \left( -\frac{\nabla^2}{2m} + V_{ex}(\mathbf{r}) \right) \Phi(\mathbf{r}) + gN \left( \Phi^* \Phi(\mathbf{r}) \right)^2.$$
 (17)

The field is here rescaled to satisfy  $\int d\mathbf{r}\Phi^*\Phi = 1$ , thus the factor N in front of the interaction term. Notice that the coupling g and the particle number N occur only in the combination gN, as opposed to the many-body description. This approximation is supposed to be valid at large particle numbers N. Minimalization of the corresponding Hamiltonian  $H_{cl} = \int d\mathbf{r} \mathcal{H}_{cl}$  leads to the non-linear Schrödinger (or Gross-Pitaevskii) equation

$$\left(-\frac{\nabla^2}{2m} + V_{ex}(\mathbf{r}) - \mu\right)\Phi(\mathbf{r}) + 2gN\Phi^*\Phi\Phi(\mathbf{r}) = 0.$$
 (18)

The chemical potential introduced is given by the normalization of  $\Phi$ . This equation can be derived from the Hartree-Fock-Bogoliubov approximation when the effect of excited particles is neglected [16].

Oscillator basis. The equation for  $\Phi$  is most easily solved introducing a harmonic oscillator basis

$$\Phi(\mathbf{r}) = \sum_{k} c_k \phi_k(\mathbf{r}). \tag{19}$$

Normalization now corresponds to  $\sum_{k} |c_{k}|^{2} = 1$ . The equation then takes the form

$$\sum_{k} (\omega_k - \mu) c_k \phi_k(\mathbf{r}) + 2gN \sum_{k,l,m} c_k^* c_l c_m \phi_k^* \phi_l \phi_m(\mathbf{r}) = 0.$$
 (20)

Multiplying with  $\phi_n^*$  and integrating we finally end up with the set of equations

$$(\omega_n - \mu)c_n + 2gN \sum_{k,l,m} c_k^* c_l c_m f_{klmn} = 0, \qquad (21)$$

where f again is the overlap integral over four harmonic oscillator eigenfunctions. The basis set is truncated at some level K, and K is raised until convergence is reached. The corresponding finite set of equations may be solved by use of the Newton-Raphson method. This method was applied in [7] for the case of a three-dimensional Bose gas. Solutions in one dimension have also been obtained earlier [6]. Again the symmetry of the ground state may be used to choose the proper subset of eigenfunctions. In one dimension we only have to consider even functions. In two dimensions only zero angular momentum eigenfunctions contribute.

Once the coefficients  $c_k$  are determined one must check if the normalization condition is satisfied. If not, a different chemical potential is chosen, and the process is repeated until normalization is obtained. Having the correct coefficients, we easily find the ground state density profile

$$\rho(\mathbf{r}) = |\sum_{k} c_k \phi_k(\mathbf{r})|^2. \tag{22}$$

In addition the ground state energy per particle reads

$$\sum_{k} \omega_k |c_k|^2 + gN \sum_{klmn} c_k^* c_l^* c_m c_n f_{klmn}. \tag{23}$$

#### 4 Numerical Results

We here present the results of the numerical diagonalization of the many-body Hamiltonian. In one dimension we have truncated the many-body basis at cutoff energy  $E_{max}=38\,\omega$ . This corresponds to a basis of up to 80524 many-body states. In two dimensions the number of overlap integrals for a given  $E_{max}$  is considerably higher than in one dimension. In addition the generation of matrix elements turns out to be very time consuming. We have therefore stopped at  $E_{max}=14\,\omega$  with a basis of up to 4532 states in two dimensions. Energies are measured in units of the oscillator frequency and lengths in units of the typical oscillator width  $1/\sqrt{m\omega}$ . g refers to the corresponding dimensionless interaction strength  $(\tilde{g}_{1D}, \tilde{g}_{2D})$  as obtained in the Appendix.

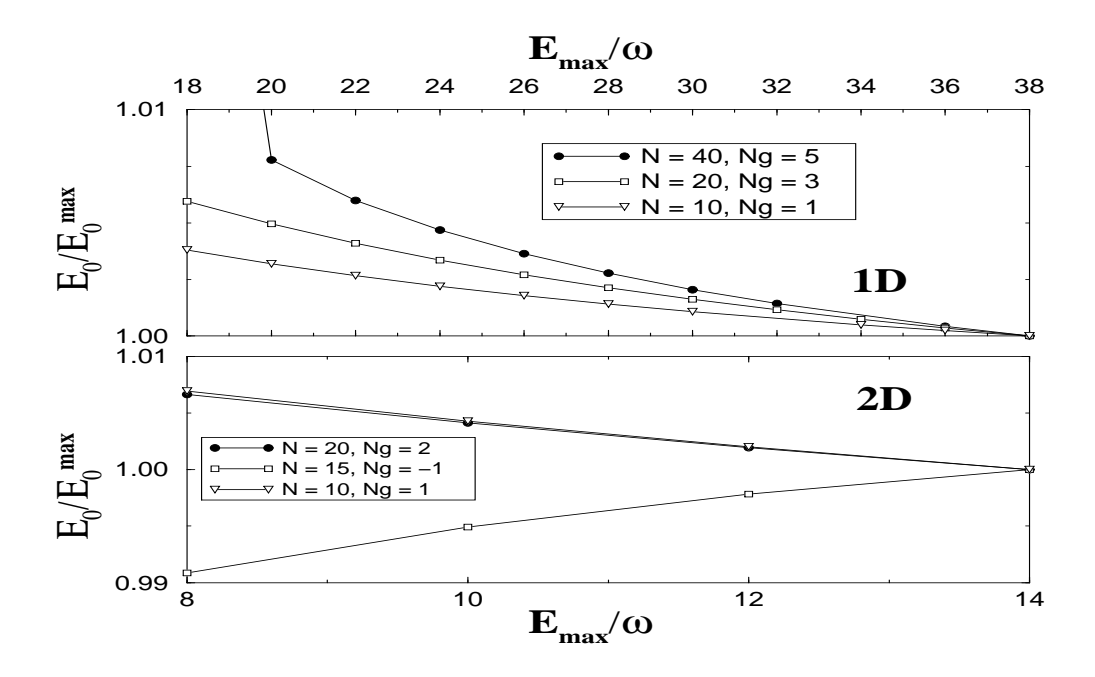


Figure 1: Convergence of the ground state energy. We plot the relative difference between the ground state energy for the given  $E_{max}$  and the energy found using the highest  $E_{max}$ . The upper graph is for one dimension and the lower for two dimensions.

In Fig. 1 we show the ground state energy as function of the cut off energy  $E_{max}$ . The plotted quantity is the ratio of the ground state energy for the given  $E_{max}$  and the energy found using the highest  $E_{max}$  considered. The upper graph is for one dimension and the lower for two dimensions. In one dimension, the relative difference in ground state energy going from  $36 \omega$  to  $38 \omega$  is seen to be about 0.05% or less. Going from  $12 \omega$  to  $14 \omega$  in two dimensions, the shift is about 0.2%. The convergence of the excitation energies is found to be considerably faster for the lowest levels, but is slower at high energy. This will be seen below in the deviation of the interaction independent energies from the exact values  $n\omega$ .

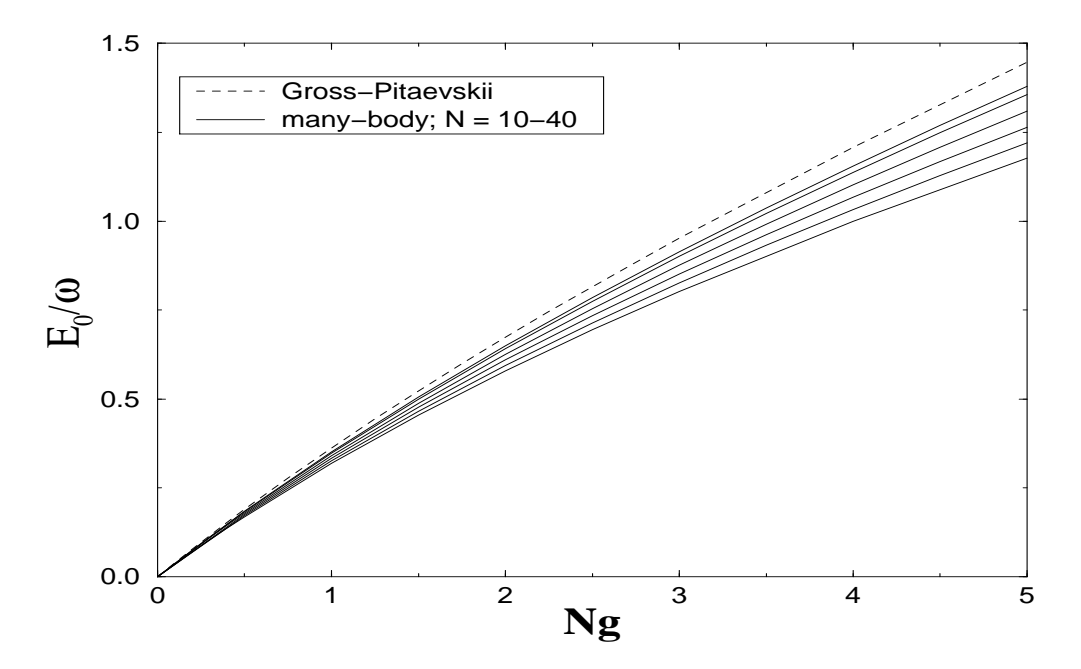


Figure 2: Ground state energy as function of interaction strength for particle numbers N = 10, 12, 15, 20, 30 and 40 in one dimension. The results of the many-body calculation approach the Gross-Pitaevskii approximation as the particle number increases.

## 4.1 Ground state energy

In this Subsection we show the effect of the interaction on the energy of the ground state. In all figures the ideal gas ground state energy is set to zero.

Linear Bose gas. Fig. 2 shows the ground state energy in one dimension, both in the GP approximation and in the many-body description. For given Ng the energy resulting from the many-body calculation is seen to approach the GP value as the particle number N is increased. The discrepancy between the approximations increases with Ng.

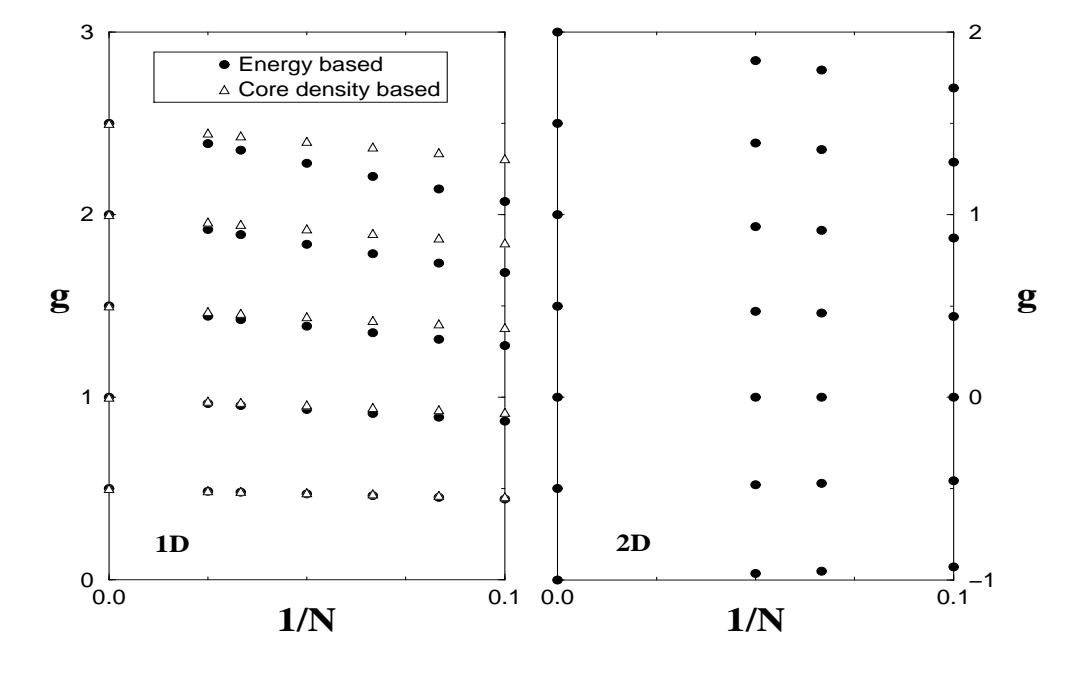


Figure 3: Effective coupling in one (left) and two (right) dimensions.

Effective coupling constant. This discrepancy should come as no surprise since we here compare the predictions of a classical mean-field theory to the exact solutions of a quantum mechanical many-body problem. In order to appreciate how well the Gross-Pitaevskii approximation works as an effective theory, we must allow for renormalization of the parameters of the theory. We will here only consider the effect of letting the coupling g become a function of the particle number N. The corrections due to finite N may then be parameterized by the expansion

$$g = g_0 + \frac{g_1}{N} + \frac{g_2}{N^2} + \cdots, (24)$$

where  $g_1$  is a function of  $g_0$  etc. The coefficients  $g_i$  are determined by fitting the results of the classical model with those of the many-body calculation. As an initial guess, we note that each particle interacts with N-1 and not N other particles. We therefore expect that the rescaling  $Ng_0 \to Ng_0(1-1/N)$  will remove the major part of the deviation between the mean field and many-body results.

Let us reconsider the ground state energy in one dimension. For a set of couplings and particle numbers we find the rescaled coupling which yields the corresponding energy given by the many-body calculation. In Fig. 3 this rescaled coupling is plotted (filled circles) as a function of 1/N for various values of the bare coupling. The bare coupling is found at 1/N = 0. For the range of parameters

considered, the dependence of the rescaled coupling on 1/N seems to be close to a linear function. Including a possible quadratic term, we write

$$g = g_0 + \frac{g_1}{N} + \frac{g_2}{N^2}. (25)$$

The coefficients  $g_1$  and  $g_2$  are determined numerically. Combining the results from the different curves, we find that the functions  $g_i(g_0)$  are well approximated by

$$g_1(g_0) = -1.04g_0 - 0.30g_0^2, (26)$$

and

$$g_2(g_0) = 0.06g_0 + 0.30g_0^2. (27)$$

The dominating correction is obviously from the shift  $N \to N-1$ .

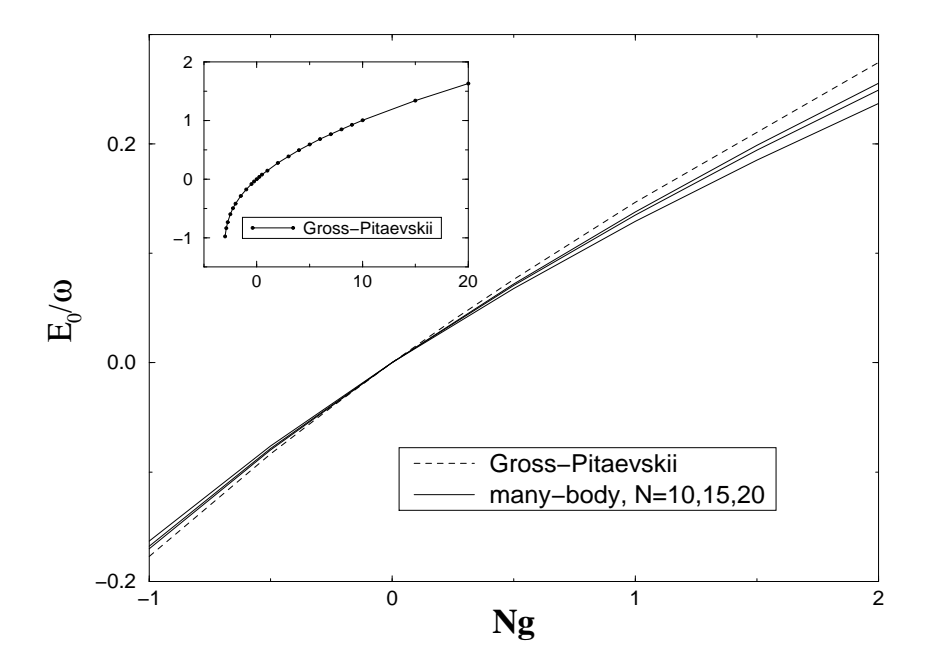


Figure 4: Ground state energy as function of interaction strength and for different particle numbers in two dimensions. The results of the many-body calculation are compared to the Gross-Pitaevskii approximation, which is approached as the particle number increases. The insertion shows the energy in the Gross-Pitaevskii approximation over a broader range of the interaction strength.

Planar Bose gas. The insertion in Fig. 4 shows the GP ground state energy in two dimensions as function of Ng. The energy falls rapidly with decreasing,

negative coupling. With a basis of up to 28 oscillator eigenfunctions, we have not been able to reach convergence near  $E_0 = -\omega$ . It seems though that  $dE_0/d(Ng)$  approaches infinity as we get closer to this point, thus indicating that no stable ground state may be formed for stronger attractive couplings. This is agreement with Pitaevskii's analysis of the system [22], where it is shown that an attractive interaction leads to collapse of the gas for energies more than  $\omega$  below the ideal gas ground state energy. Similar conclusions are drawn in [23].

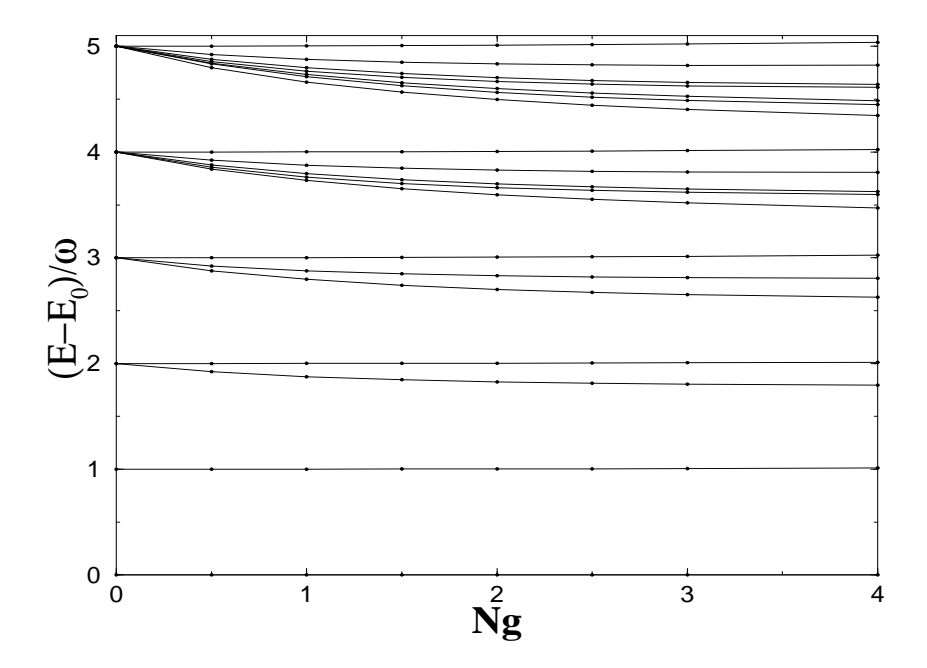


Figure 5: Excitation energies in a one-dimensional system of 30 bosons as function of the interaction strength.

The Gross-Pitaevskii ground state energy is in Fig. 4 also plotted together with the results of the many-body calculation for N=10,15 and 20. Again the GP-approximation is approached as N increases. As for one dimension, we have calculated the effective coupling which, used in the GP-approximation reproduces the energy obtained in the many-body calculation. This effective coupling is plotted at the right hand side of Fig. 3. Fitting the curves with a linear function of 1/N, we find that they may be approximated by the formula

$$g = g_0 \left( 1 - \frac{1 + 0.3g_0}{N} \right). \tag{28}$$

Note that this is the same as the 1/N-correction i one dimension. Again,  $N \to N-1$  is the most important effect.

#### 4.2 Excitations

In Section 2 we saw that the excitation energies must consist of ladders with energy spacing  $\omega$ . This is due to the existence of the collective raising operator  $A^{\dagger}$ . The bottom of each of the ladders must however be determined by other means, and we here present the results of the numerical diagonalization of the many-body Hamiltonian.

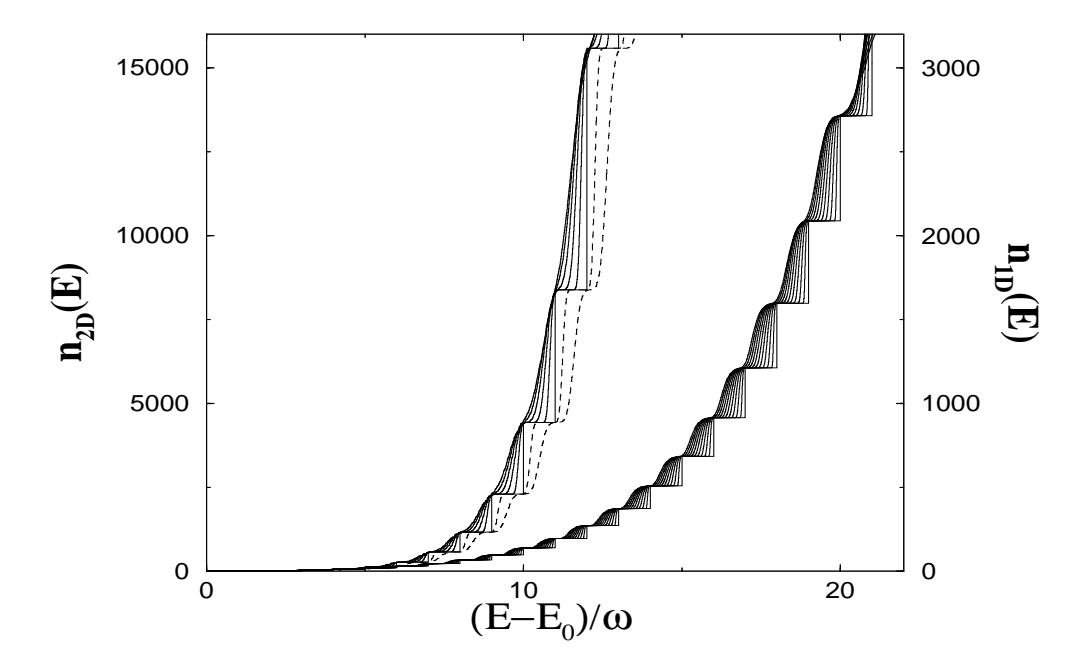


Figure 6: Summed density of states in a one- (right curves) and two-dimensional (left curves) system of 20 and 15 bosons respectively. The interaction strength is in the range Ng = 0, ..., 2 in one dimension and Ng = -1, ..., 2.5 in two dimensions. Ng increases from right to left, and negative interaction strengths are indicated by dashed lines.

Linear Bose gas. In Fig. 5 the lowest excitation energies in one dimension are given as function of Ng for the case of 30 particles. The degeneracy at zero coupling is split by the interaction. For each level in the ideal case, one level remains independent of the coupling. These levels correspond to excitations described by  $A^{\dagger}$  from the ground state. The others spread out below, and above each of these we find the mentioned ladder of levels. Similar results are obtained for N=10,12,15,20 and 40. The relative shift in the energies going from N=10 to N=40 with a given Ng is less than 1% for the range of parameters presented in Fig. 5.

The splitting of the degeneracy by the interaction leads to a more even distribution of energy levels than in the free case. As an illustration of this, Fig. 6 shows the number of energy levels  $n_{1D}(E)$  (right curves) below a given energy

E measured from the ground state. We have taken N=20, and the coupling ranges from Ng=0-2 in steps of 0.2. This summed density of states is indeed smoothed by the presence of the interaction. Note that the curves coincide at points  $(E-E_0)/\omega = n$ . This happens because all interaction-dependent excitation energies lie in the gap below the corresponding undisturbed level for the considered values of the coupling.

Planar Bose gas. The lowest energy levels of a planar system with 20 bosons

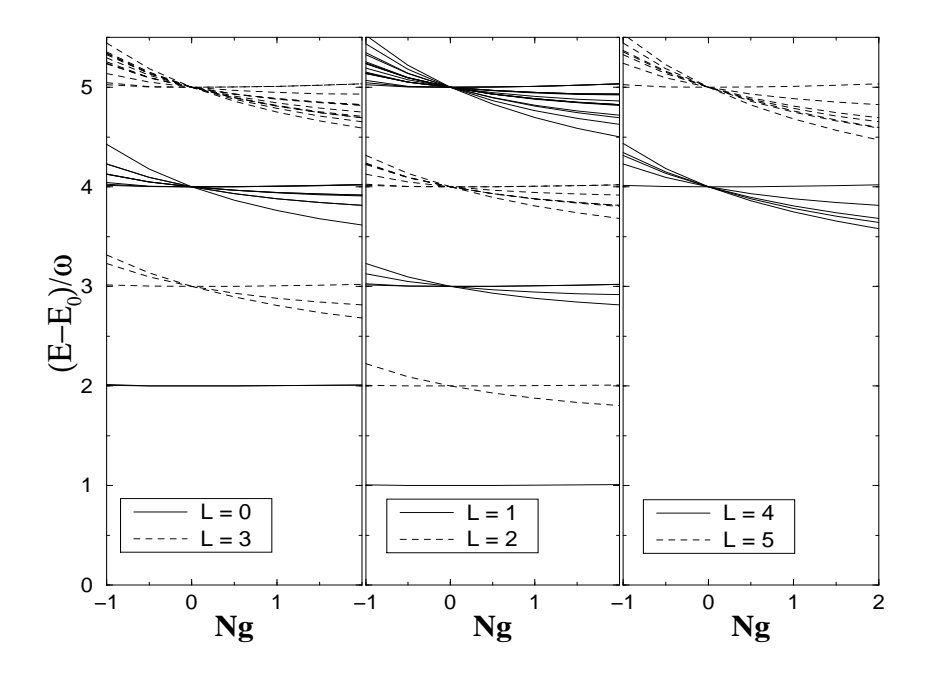


Figure 7: Excitation energies in a two-dimensional system of 20 bosons as function of the interaction strength. L is the angular momentum.

are given in Fig. 7 as function of the dimensionless coupling. For each level with non-zero angular momentum L, there is a level with the same energy and angular momentum -L. The degeneracy at g=0 is broken for non-zero g, but again there are levels which are unaffected by the interaction. In dimensionless units, these have the same energy and angular momentum. Above each energy level there is a ladder of levels with energy and angular momentum increasing in steps of unity.

In Fig. 6 the corresponding summed density of states  $n_{2D}(E)$  (left curves) is plotted for 15 bosons with the coupling running from Ng = -1 to 2 in steps of 0.5. Levels for both positive and negative angular momentum are included. The step-like form of the curve for the free case is again smoothed by the interaction.

For stronger couplings we do not quite reproduce the independence of the interaction. This is due to the truncation of the basis of states. However, since

we know that these levels must approach  $(E-E_0)/\omega$  = integer as the basis set is increased, the deviation gives a good indication of the accuracy of the results.

#### 4.3 Ground state density

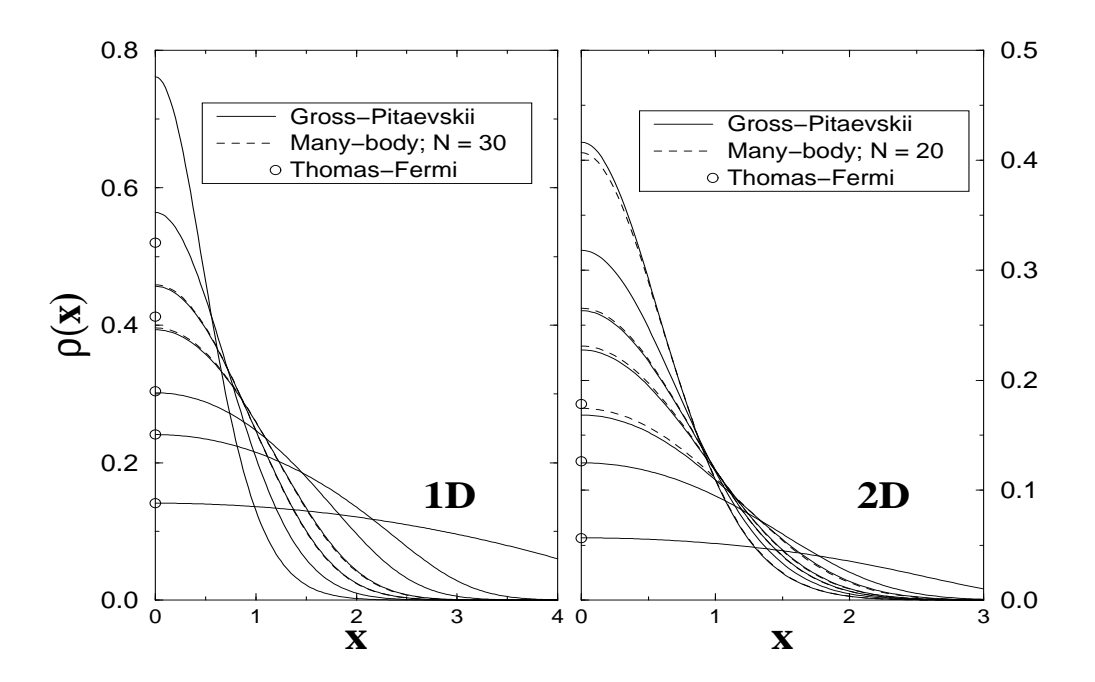


Figure 8: Normalized ground state density in one (left) and two dimensions (right). The density is plotted as function of the dimensionless radius  $x = r\sqrt{m\omega}$ . The solid curves give the density in the Gross-Pitaevskii approximation for Ng = -1, 0, 1, 2, 5, 10 and 50. The circles on the vertical axis show the corresponding core density as given in the Thomas-Fermi (TF) approximation for repulsive interaction. The core density is lowered with increasing interaction strength. From the many-body calculation we have obtained the density represented by dashed lines. We have used N = 30 in one dimension and N = 20 in two dimensions.

The ground state can in the GP-approximation be written as a superposition of oscillator functions with even parity or zero angular momentum in one and two dimensions respectively. In the many-body description this is no longer true, and single particle states with other quantum numbers will contribute. We here show how this affects the ground state density.

Ground state density profile. For large gN the interaction energy dominates the kinetic energy, and one may neglect the kinetic term in the GP-equation.

This is the Thomas-Fermi (TF) approximation [3]. The solution is now simply

$$|\Phi(\mathbf{r})|^2 = \frac{1}{2gN} (\mu - V_{ex}(\mathbf{r})) \theta (\mu - V_{ex}(\mathbf{r}))$$

$$\equiv \frac{m\omega^2}{4gN} (R^2 - r^2) \theta (R^2 - r^2). \tag{29}$$

This describes a condensate density which vanishes outside the radius  $R = \sqrt{2\mu/m\omega^2}$ . We here compare the normalized core density  $\rho(0) = \mu/2gN$  in the TF-approximation with the exact solution of the Gross-Pitaevskii approximation, and also with the full many-body calculation. The TF-approximation in three dimensions has been studied earlier in [5].

In Fig. 8 we plot the normalized ground state density  $\rho(x)$  as function of the dimensionless radius  $x = r\sqrt{m\omega}$  in one and two dimensions. The core density in the TF-approximation is shown as circles on the vertical axis. This approximation seems to work well for interaction strengths above  $Ng \sim 5$  in one dimension and above  $Ng \sim 10$  in two dimensions. For the lowest values of the interaction strength we compare the Gross-Pitaevskii approximation to the full many-body calculation with N=30 and N=20 in one and two dimensions respectively. The GP-approximation yields quite good result, especially at large distances. Let us, however study the core density more closely.

Core density: Linear Bose gas. Fig. 9 shows the normalized core density in one dimension as function of Ng. As N is increased, the result in the GP-approximation (dotted line) is approached by the results of the many-body calculation. The deviation is seen to increase with the interaction strength. As for the ground state energy we may correct the GP-results by introducing an N-dependent coupling. Applying the effective couplings found above, in the GP-approximation, we do however not reproduce the core densities predicted by the many-body calculation. When we instead use the density data as a basis for determining the effective couplings, we obtain the results marked by triangles in Fig. 3. They are certainly different from the couplings based on the ground state energy, and a linear estimate yields  $g = g_0(1 - 0.8/N)$ . Thus, the simple effective mean field theory with an N-dependent interaction strength cannot account for all many-body effects in the ground state.

Planar Bose gas. The normalized core density in two dimensions is also plotted in Fig. 9. The N-dependence of the many-body results is by far strongest for negative coupling, and again the GP-results are approached as N increases. A rescaling of the coupling shows that  $g \to g(1-1/N)$  compensates for the major part of the deviation also in this case.

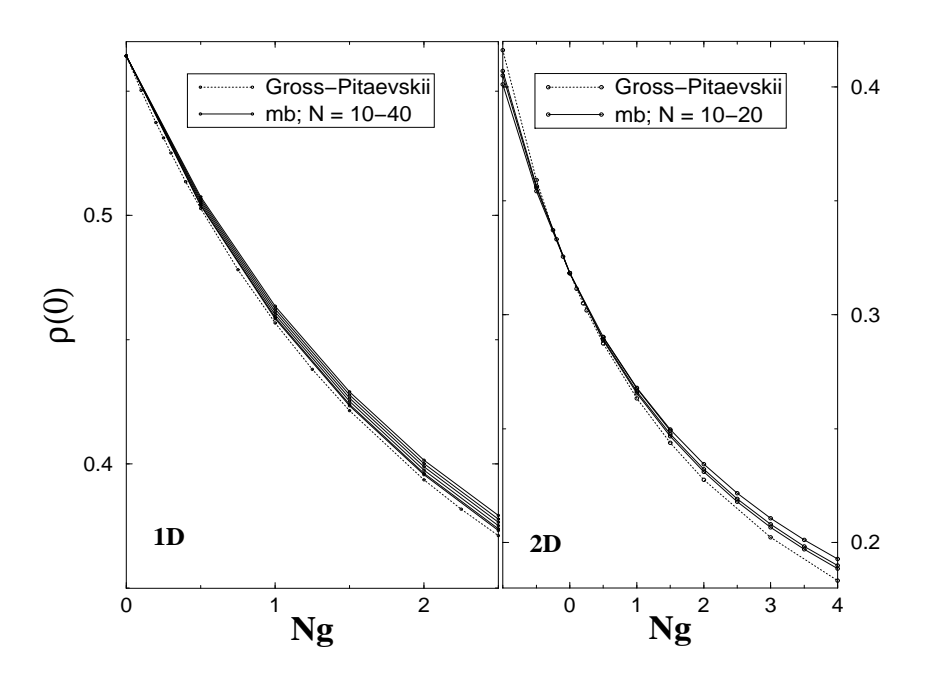


Figure 9: Normalized core density in one (left) and two dimensions (right). The result of the many-body calculation (mb) is plotted as function of the interaction strength for different particle numbers and is compared to the Gross-Pitaevskii approximation. The particle numbers are 10, 12, 15, 20, 30 and 40 in one dimension and 10, 15 and 20 in two dimensions. In both cases, N increases from above for positive q.

## 4.4 Specific heat.

Having obtained the lowest excitation energies of the system of trapped bosons, it is straightforward to find the partition function and the thermodynamical quantities one may derive thereof. The validity of these results is limited to low temperatures  $T \ll E_{max}$ . Just how low the temperature must be will be clear in the examples following.

Let us first consider the one-dimensional system. With 20 particles and a cutoff at  $E_{max} = 26 \,\omega$  we find the specific heat plotted in the left graph of Fig. 10.
The coupling ranges from Ng = 0 to 2 in steps of 0.5, starting from below at low
temperatures. The dotted line is the specific heat for 20 non-interacting bosons
calculated in the canonical ensemble [24]. We also show the result of a calculation
in the grand canonical ensemble. For particle numbers as low as this, the two
ensembles predict somewhat different specific heats. The exact curve agrees with
the curve for g = 0 up to a temperature around 1.5  $\omega$ . At higher temperatures
the many-body calculation breaks down. For temperatures where the results are
valid we find that the repulsive interaction yields a higher specific heat than in
the case of non-interacting particles. This happens because the interaction brings
most of the energy levels closer to the ground state. The effect of the interaction

grows with increasing temperature in this regime.

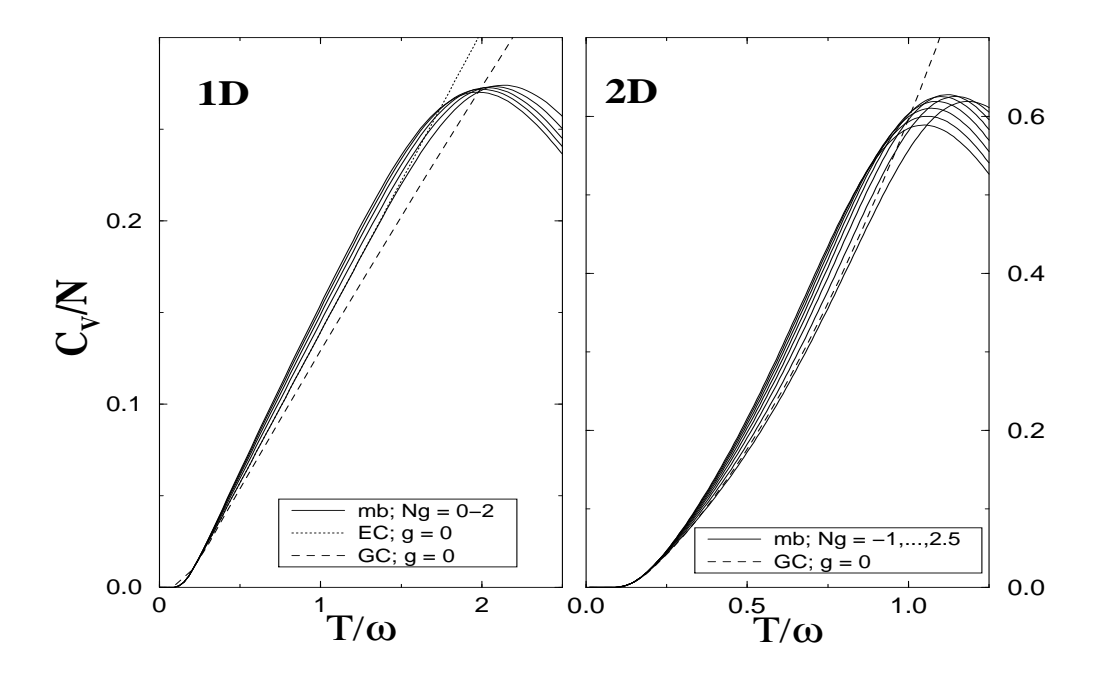


Figure 10: Specific heat per particle for a one- (left) and two-dimensional (right) system of 20 and 15 bosons respectively. The specific heat is plotted as function of the reduced temperature  $T/\omega$ . In one dimension the interaction strength runs from Ng=0 to 2 and in two dimensions from -1 to 2.5, both in steps of 0.5. The many-body results (mb) are compared to the curve for the ideal gas as given in the grand canonical ensemble (GC). In one dimension we also show the exact result in the canonical ensemble (EC). We have set  $k_B=1$ .

We have also calculated the specific heat for a two-dimensional system of 15 bosons. The cut-off is here  $E_{max} = 14 \,\omega$ , and the basis thus contains states with angular momentum up to  $L = \pm 14$ . This specific heat is shown in the right graph of Fig. 10. The calculation now breaks down around  $T/\omega = 1$ . For comparison we have included the specific heat of 15 non-interacting bosons as given in the grand canonical ensemble. Again a repulsive interaction increases the specific heat, while it is decreased in the attractive case.

## 5 Discussion and Conclusion

We have in this paper we presented results of many-body calculations on systems with 10 to 40 interacting bosons confined to harmonic traps in one and two dimensions. By use of a set of many-body states and decomposition of the fields in harmonic modes, we have diagonalized the Hamiltonian numerically. The resulting ground state properties have been compared to the predictions of the Gross-Pitaevskii equation, and we have found that the latter tends to over-

estimate the effects of the interaction, both for the repulsive and the attractive case. The deviation decreases with increasing particle number. We have tried to compensate by introducing an effective interaction strength in the mean-field description. However, rescaling based on ground state energy and core density separately result in different effective couplings. The effective theory is therefore too simple, and needs to be extended.

We have also considered the lowest excitation energies. In both one and two dimensions we have reproduced the interaction independent levels which must be present in these systems [13]. The interaction breaks the high degree of degeneracy in the non-interacting gas, and the summed density of states looses some of its step-like shape. We have also calculated the specific heat based on these excitation energies. For low temperatures, where the results are valid, the repulsive interaction increases the specific heat, while it is decreased in the attractive case.

It would be interesting to compare the obtained excitation energies with the results of a calculation based on the Bogoliubov approximation. One might also use the obtained density of states as a basis for calculations in the microcanonical ensemble.

#### Acknowledgments

The authors would like to thank F. Ravndal for bringing their attention to this problem and for useful comments and suggestions. S. B. Isakov is acknowledged for useful discussions and for informing us about reference [13].

## A Effective coupling in lower dimensions

Inspired by proposed experiments in lower dimensions [25, 26], we will here consider the effect of having a strongly anisotropic trapping potential. Assuming  $\omega_z \ll \omega_{x,y}$  or  $\omega_z \gg \omega_{x,y}$  the system should effectively be one- or two-dimensional. When the larger oscillator energy dominates all other energies in the system, we may assume that there will be no excitations in this direction. This means that the field operator may be written as

$$\hat{\Psi}(x,y,z) = \sum_{k} \phi_0(x)\phi_0(y)\phi_k(z)a_{00k}$$
(30)

for the one dimensional case, and

$$\hat{\Psi}(x,y,z) = \sum_{k} \phi_0(z)\phi_k(x,y)a_{0k}$$
(31)

for the two-dimensional one. We may then integrate over the spatial variables corresponding to the stronger oscillation frequencies. This results in a rescaling

of the coupling constant g in Eq. (2). In the two-dimensional theory we find

$$g_{2D} = g_{3D} \sqrt{\frac{m\omega_z}{2\pi}}. (32)$$

In one dimension the coupling becomes

$$g_{1D} = g_{3D} \frac{m\omega_{xy}}{2}. (33)$$

Measuring energy in units of the remaining oscillator frequency  $\omega$  and lengths in units of the oscillator length  $1/\sqrt{m\omega}$  we obtain the dimensionless coupling constants

$$\tilde{g}_{2D} = \sqrt{2\pi} \frac{a}{a_z},\tag{34}$$

and

$$\tilde{g}_{1D} = \pi \sqrt{\frac{\omega_{xy}}{\omega_z}} \frac{a}{a_{xy}},\tag{35}$$

where  $a_i = \sqrt{\hbar/m\omega_i}$  and  $a = mg_{3D}/2\pi\hbar^2$ . We have here reintroduced  $\hbar$ . The effective coupling is seen to increase with the strength of the stronger oscillator frequency. This is an effect of reducing the length in which the particle density may extend in the dimensions integrated out.

As an example of a possible physical realization, we mention that Ketterle and van Druten [25] have suggested an experiment with  $\omega_z/\omega_{xy} \sim 10^{-3}$  and  $\omega_{xy} \sim 200nK$ . With a scattering length of typically 100 Bohr radii, this yields an effective one-dimensional coupling  $\tilde{g}_{1D} \sim 1$ . This corresponds to a strong coupling system for any finite number of particles. Other configurations may yield a weaker effective coupling.

## References

- K.B. Davis, M.-O. Mewes, M.R. Andrews, N.J. van Druten, D.S. Durfee, D.M. Kurn, and W. Ketterle, Phys. Rev. Lett. 75, 3969 (1995).
- [2] M. H. Anderson, J. R. Ensher, M. R. Matthews, C. E. Wieman and E. A. Cornell, Science 269, 198 (1995).
- [3] G. Baym and C. Pethick, Phys. Rev. Lett. 76, 6 (1996).
- [4] K. G. Singh and D. S. Rokhsar, Phys. Rev. Lett. 77, 1667 (1996).
- [5] M. Edwards et al., Phys. Rev. A 53, R1950 (1996).

- [6] P. A. Ruprecht, M. J. Holland, K. Burnett and M. Edwards, Phys. Rev. A 51, 4704 (1995).
- [7] M. Edwards *et al.*, Phys. Rev. Lett. **77**, 1671 (1996).
- [8] F. Dalfovo et al., unpublished (cond-mat/9705240).
- [9] B. D. Esry, Phys. Rev. A 55, 1147 (1997).
- [10] D. S. Jin et al., Phys. Rev. Lett. 77, 420 (1996).
- [11] M.-O. Mewes et al., Phys. Rev. Lett 77, 988 (1996).
- [12] S. Stringari, Phys. Rev. Lett. 77, 2360 (1996).
- [13] A. L. Fetter and D. S. Rokhsar, unpublished (cond-mat/9704234).
- [14] E. P. Gross, Nuovo Cimento **20**, 454 (1961); J. Math. Phys. **46**, 137 (1963).
- [15] L. P. Pitaevskii, Zh. Eksp. Teor. Fiz. 40, 646 (1961); Sov. Phys.-JETP 13, 451 (1961).
- [16] A. Griffin, Phys. Rev. B **53**, 9341 (1996).
- [17] I. S. Gradshteyn and I. M. Rhyzhik, *Table of Integrals, Series and Products* (Academic Press, New York, 1965).
- [18] C. Lanczos, J. Res. Nat. Bur. Standards 45, 255 (1950).
- [19] H. Bethe, Z. Physik **71**, 205 (1931).
- [20] E. H. Lieb and W. Liniger, Phys. Rev. 130, 1605 (1963); E. H. Lieb, ibid., 1616.
- [21] C. N. Yang and C. P. Yang, J. Math. Phys. 10, 1115 (1969).
- [22] L. P. Pitaevskii, unpublished (cond-mat/9605119).
- [23] K. Watanabe, T. Mukai and T. Mukai, Phys. Rev. A 55, 3639 (1997).
- [24] T. Haugset, H. Haugerud and J. O. Andersen, Phys. Rev. A 55, 2922 (1997).
- [25] W. Ketterle and N. J. van Druten, Phys. Rev. A 54, 656 (1996).
- [26] T. Pfau and J. Mlynek, OSA Trends in Optics and Photonic Series 7, 33 (1997).